Fassan, M., Barbareschi, M., Galligioni, E., Gasparini, P., Baldassarre, G., Croce, CM., Vecchione, A. LZTS1 downregulation confers paclitaxel resistance and is associated with worse prognosis in breast cancer. *Oncotarget*, 28;5(4):970-977, 2014.

12） Tamari, K., Hayashi, K., Ishii, H., Kano, Y., Konno, M., Kawamoto, K., Nishida, N., Koseki, J., Fukusumi, T., Hasegawa, S., Ogawa, H., Hamabe, A., Miyo, M., Noguchi, K., Seo, Y., Doki, Y., Mori, M., Ogawa, K. Identification of chemoradiation-resistant osteosarcoma stem cells using an imaging system for proteasome activity. *Int. J. Oncol.*, 45(6):2349-2354,2014.

13） Hayashi, K., Tamari, K., Ishii, H., Konno, M., Nishida, N., Kawamoto, K., Koseki, J., Fukusumi, T., Kano, Y., Nishikawa, S., Miyo, M., Noguchi, K., Ogawa, H., Hamabe, A., Seo, Y., Doki, Y., Mori, M., Ogawa, K. Visualization and characterization of cancer stem-like cells in cervical cancer. *Int. J. Oncol.*, 45(6):2468-2474,2014.

14） Colvin, S. H., Nishida, N., Koseki, J., Konno, M., Kawamoto, K., Tsunekuni, K., Doki, Y., Mori, M., Ishii, H. Cancer Stem Cells of the Digestive System. *Jpn. J. Clin. Oncol.* 44(12):1141-1149,2014.

15） Koga, C., Kobayashi, S., Nagano, H., Tomimaru, Y., Hama, N., Wada, H., Kawamoto, K., Eguchi, H., Konno, M., Ishii, H., Umeshita, K., Doki, Y., Mori, M. Reprogramming Using microRNA-302 Improves Drug Sensitivity in Hepatocellular Carcinoma Cells. *Ann. Surg. Oncol.*, Suppl 4:S591-600,2014.

16） Kawamoto, K., Yabe, S., Konno, M., Ishii, H., Nishida, N., Koseki, J., Fukuda, S., Tomimaru, Y., Hama, N., Wada, H., Kobayashi, S., Eguchi, H., Tanemura, M., Ito, T., Lee, EY., Mukai, E., Miki, T., Doki, Y., Mori, M., Hamazaki, TS., Nagano, H., Okochi, H. NeuroD1 with conditioned medium efficiently induce ASC to insulin-producing cells both in vitro and in vivo. *J. Stem Cell Res. Ther.*, 2014. (in press)

17） Nishikawa, S., Konno, M., Hamabe, A., Hasegawa, S., Kano, Y., Fukusumi, T., Sato, T., Takiguchi, S. Mori, M. Doki, Y. Ishii, H. Surgically Resected Human Tumors Reveal the Biological Significance of the Gastric Cancer Stem Cell Markers CD44 and CD26. *Int. J. Oncol.* 2014. (in press)

18） Miyazaki, S., Yamamoto, H., Miyoshi, N., Wu, Xin., Ogawa, H., Uemura, M. Nishimura, J., Hata, T., Takemasa, I., Mizushima, T., Konno, M., Doki, Y., Mori, M., Ishii, H. A Cancer Reprogramming Method Using MicroRNAs as a Novel Therapeutic Approach against Colon Cancer. *Ann. Surg. Oncol.* 2014. (in press)

19） Ogawa, H., Nagano, H., Konno, M., Eguchi, H., Koseki, J., Kawamoto, K., Nishida, N., Colvin, S. H., Tomokuni, A., Tomimaru, Y., Hama, N., Wada, H., Marubashi, S., Kobayashi, S., Mori, M., Doki, Y., Ishii, H. The combination of the expression of hexokinase 2 and pyruvate kinase M2 is a prognostic marker in patients with pancreatic cancer. *Mol. Clin. Oncol.* 2014. (in press)

2. 学会発表

1） 石井秀始：Innvovative Medicine for Gastrointestinal Cancer Stem Cells、第 52 回日本癌治療学会学術集会、2014 年 8 月 28 日～30 日、横浜

2） 石井秀始：創薬標的としての癌幹細胞エピゲノム代謝、第 73 回日本癌学会学術総会、2014 年 9 月 25 日~27 日、横浜

3） 石井秀始、他：難治性消化器癌に対する革新的治療法、第 73 回日本癌学会学術総会、2014 年 9 月 25 日~27 日、横浜

4） 石井秀始：Innovative drug discovery for intractable cancer stem cells、第 76 回日本血液学会学術集会、2014 年 10 月 31 日~11 月 2 日、大阪

5) 石井秀始：がん幹細胞を標的としたが
ん治療、第 27 回日本バイオセラピイ
学会学術集会総会、2014 年 12 月 4 日
〜12 月 5 日、大阪

G．知的財産権の出願・登録状況
（予定を含む。）

1.特許取得

1) 発明の名称：マイクロ RNA における
メチル化修飾部位を計測する方法
発明者：石井秀始、森正樹、土岐祐一
郎、西田尚弘、今野雅允、小関準、川
本弘一、大房健、近藤礎、中村眞
出願人：いであ株式会社、株式会社エ
バンス、国立大学法人大阪大学
出願番号：特願 2014-266607
出願日：平成 26 年(2014 年)12 月 26 日

2) 発明の名称：多能性幹細胞の品質診断
方法及び診断キット、抗がん剤並びに
疾患モデル動物
発明者：石井秀始、森正樹、土岐祐一
郎、今野雅允、川本弘一、西田尚弘、
小関準、新井貴博、佐藤暢彦、近藤礎、
中村眞
出願人：ユニーテック株式会社、株式
会社エバンス、国立大学法人大阪大学
出願番号：特願 2014-266696
出願日：平成 26 年(2014 年)12 月 26 日

3) 発明の名称：膵癌治療感受性の診断方
法及び膵癌治療感受性の増強剤
発明者：石井秀始、永野浩昭、森正樹、
土岐祐一郎、今野雅允、江口英利、川
本弘一、西田尚弘、小関準、長谷川慎
一郎、野口幸蔵、近藤礎、中村眞
出願人：株式会社エバンス、国立大学
法人大阪大学
出願番号：特願 2014-266697
出願日：平成 26 年(2014 年)12 月 26 日

2.実用新案登録
特になし。

3.その他
特になし。

様式第19

<div align="center">学 会 等 発 表 実 績</div>

委託業務題目「　固形がん幹細胞を標的とした革新的治療法の開発に関する研究　」
機関名　国立大学法人大阪大学大学院医学系研究科

１．学会等における口頭・ポスター発表

発表した成果（発表題目、口頭・ポスター発表の別）	発表者氏名	発表した場所（学会等名）	発表した時期	国内・外の別
モーニングセミナー（肝胆膵領域癌におけるマイクロRNA研究の意義）	森正樹	和歌山（第26回日本肝胆膵外科学会学術集会）	2014年6月11日〜6月13日	国内
座長（骨転移の病態と最新治療）	森正樹	石川（第23回日本がん転移学会学術集会・総会）	2014年7月10日〜7月11日	国内
学術セミナー（癌幹細胞研究の現状と展望）	森正樹	神奈川（第52回日本癌治療学会学術集会）	2014年8月28日〜8月30日	国内
招待講演(未来の医療を変えるナノDDS〜あらゆる微小空間で生体機能をコントロールする革新技術の創製〜)	片岡一則	東京（2014年度グレーター東大塾 超高齢社会日本を支える医療技術と社会システム）	2014年5月14日	国内
招待講演（高分子ナノテクノロジーによる標的指向型創薬）	片岡一則	福岡（第55回日本神経学会学術大会）	2014年5月21日	国内
特別講演（ナノマテリアルから拡がる医療イノベーション- 高分子ミセルによるがんの標的治療 - ）	片岡一則	兵庫（第41回日本毒性学会学術年会）	2014年7月2日	国内
招待講演（Nanomaterials as 'the magic bullet' to eradicate cancer）	K. Kataoka	Tokyo（The 15th Anniversary Symposium of Science and Technology og Advanced Materials）	2014年7月3日	国内
招待講演（Targeted chemo- and molecular-therapy by self-assembled supramolecular nanosystems from functionalized block copolymers）	K. Kataoka	Australia（NanoBio Australia 2014 5th International NanoBio Conference & 3rd International Conference on BioNano Innovation (ICBNI)）	2014年7月8日	国外
招待講演（スマートライフケア社会への変革を先導するナノバイオテクノロジー〜あらゆる微小空間で生体機能をコントロールする革新技術の創製〜）	片岡一則	東京（実験動物中央研究所 平成26年度(第33回)学術懇話会）	2014年7月24日	国外
総会講演（Targeted chemo- and molecular-therapy by self-assembled supramolecular nanosystems from functionalized block copolymers）	K. Kataoka	USA（ISACS15 Challenges in Nanoscience）	2014年8月18日	国外
招待講演（未来の医療を変えるナノDDS〜あらゆる微小空間で生体機能をコントロールする革新技術の創製〜）	片岡一則	千葉（東大柏ベンチャープラザ10周年記念）	2014年9月4日	国外
招待講演（Block copolymer micelles as smart nanosystems for targeted drug delivery）	K. Kataoka	USA（MGH-UTokyo Symposium 2014 "Frontiers in Biomedical Engineering"）	2014年9月24日	国外
招待講演（スマートライフケア社会への変革を先導するナノバイオテクノロジー〜あらゆる微小空間で生体機能をコントロールする革新技術の創製〜）	片岡一則	神奈川（三井業最研究所 第16回最先端材料技術調査研究委員会）	2014年9月30日	国外
招待講演（Block copolymer micelles as smart nanosystems for targeted drug delivery）	K. Kataoka	Hyogo（11th France-Japan DDS Symposium "Recent Achievements and Further Challenges in Drug Delivery Research"）	2014年10月8日	国内
招待講演（Smart targeted therapy by self-assembled supramolecular nanosystems）	K. Kataoka	Tokyo（JSPS A3 Foresight International Symposium on Nano-Biomaterials and Regenerative Medicine）	2014年10月9日	国内

教育講演（超分子ナノマシンによる薬物・遺伝子のピンポイントデリバリー）	片岡一則	神奈川（第79回日本泌尿器科学会東部総会）	2014年10月14日	国内
特別講演（ナノテクノロジーで創る魔法の弾丸～がんの標的治療への挑戦～）	片岡一則	東京（第42回日本潰瘍学会）	2014年11月1日	国内
招待講演（Nanotechnology to develop "the magic bullet" for targeted cancer therapy）	K. Kataoka	Fukuoka（27th International Microprocesses and Nanotechnology Conference (MNC 2014)）	2014年11月5日	国内
招待講演（Smart targeted therapy by self-assembled supramolecular nanosystems）	片岡一則	京都（第30回(2014)京都賞記念ワークショップ先端技術部門「バイオマテリアル研究の最前線」）	2014年11月12日	国内
招待講演（Targeted chemo- and molecular-therapy by self-assembled supramolecular nanomedicines）	K. Kataoka	Ibaraki（The 10th International Polymer Conference IPC2014）	2014年12月4日	国内
招待講演（高分子ミセル医薬：その特徴と将来展望）	片岡一則	東京（日本DDS学会創立30周年シンポジウム）	2014年12月15日	国内
基調講演（Block copolymer micelles as smart nanosystems for drug targeting）	K. Kataoka	China（The 1st International Symposium on Translational Nanomedicine）	2015年1月9日	国外
基調講演（ナノDDS技術による均質・高付加価値な難病治療・再生医療の実現）	片岡一則	愛知（第3回 国際先端生物学・医学・工学会議 (ICIBME 2015)）	2015年1月15日	国内
招待講演（未来の医療を変えるナノDDS ～あらゆる微小空間で生体機能をコントロールする革新技術の創製～）	片岡一則	東京（新春特別講演会「未踏科学技術2015」）	2015年1月20日	国内
Invited Lecture（"Development of supramolecular nanocarriers for cancer diagnosis and therapy"）	N. Nishiyama	Korea（Emerging Biomaterials 2014 (23 May)）	2014年5月23日	国外
シンポジスト（"がんの診断・治療のための高分子ミセル型DDSの開発"）	西山伸宏	宮城（日本病院薬剤師会東北ブロック第4回学術大会）	2014年5月31日	国内
招待講演（"高分子ナノテクノロジーを基盤とするナノ医薬品の開発"）	西山伸宏	東京（第10回つくばがん遺伝子治療研究会）	2014年6月20日	国内
Invited Lecture（"Biological functionalities of polymeric micelle systems for targeting cancer"）	N. Nishiyama	Switzerland（The European Summit for Clinical Nanomedicine 2014 (6th CLINAM 2014)）	2014年6月23日	国外
招待講演（"高分子ミセル型ナノ医薬品の研究開発"）	西山伸宏	京都（第12回技術講演会）	2014年7月16日	国内
シンポジスト（"生体イメージングを活用したナノDDS設計", 3S05a疾患克服を目指したケミカルバイオフォトニクス技術）	西山伸宏	京都（第87回日本生化学会大会）	2014年10月17日	国内
基調講演(がん幹細胞を標的とした治療戦略)	佐谷秀行	宮城（第18回日本がん分子標的治療学会学術集会）	2014年6月25日	国内
JSH-JCA Joint Symposium（Redox regulation in cancer stem cells.）	Saya H	Osaka（"Metabolomics and therapeutic strategy in myeloid and other tumors" The 76the Annual Meeting of the Japanese Society of Hematology.）	2014年11月2日	国内
ポスター（"Identification of microRNA-27b as a master regulator generating breast cancer stem cells"）	Ryou-u Takahashi, Hiroaki Miyazaki, Takahiro Ochiya	ドイツ（EMBL）	2014年5月8日	国外

講演（乳がんにおける幹細胞形質を制御する因子の同定とその機能解析）	高橋陵宇, 宮崎裕明, 竹下文隆, 小野麻紀子, 田村研治, 落谷孝広	神奈川（第73回日本癌学会学術総会）	2014年9月25日	国内
シンポジスト（"Loss of MicroRNA-27b-mediated Gene Repression Promotes Generation of Breast Cancer Stem Cells"）	Ryou-u Takahashi, Hiroaki Miyazaki, Takahiro Ochiya	ギリシャ（19th World Congress on Advances in Oncology and 17th International Symposium on Molecular Medicine）	2014年10月10日	国外
招待講演（Dissecting cancer biology by studying induced pluripotency）	Yamada, Y.	China(Nuclear Reprogramming and the Cancer Genome 2014)	2014年10月31日～11月2日	国外
招待講演（Understanding Pediatric Cancer Development by Studying Induced Pluripotency）	Yamada, Y.	Germany(ADVANCES IN NEUROBLASTOMA RESEARCH)	2014年5月13日～5月16日	国外
招待講演（Dissecting cancer biology by studying induced pluripotency）	Yamada, Y.	Korea（8th International Cell Therapy Conference）	2014年10月23日	国外
シンポジウム（Innovative Medicine for Gastrointestinal Cancer Stem Cells）	石井秀始	神奈川（第52回日本癌治療学会学術集会）	2014年8月28日～8月30日	国内
ランチョンセミナー（創薬標的としての癌幹細胞エピゲノム代謝）	石井秀始	神奈川（第73回日本癌学会学術総会）	2014年9月25日～9月27日	国内
シンポジウム（難治性消化器癌に対する革新的治療法）	石井秀始、森正樹、土岐祐一郎	神奈川（第73回日本癌学会学術総会）	2014年9月25日～9月27日	国内
シンポジウム（Innovative drug discovery for intractable cancer stem cells）	石井秀始	大阪（第76回日本血液学会学術集会）	2014年10月31日～11月2日	国内
シンポジウム（がん幹細胞を標的としたがん治療）	石井秀始	大阪（第27回日本バイオセラピイ学会学術集会総会）	2014年12月4日～12月5日	国内

２．学会誌・雑誌等における論文掲載

掲載した論文（発表題目）	発表者氏名	発表した場所 （学会誌・雑誌等名）	発表した時期	国内・外の別
Ultra-sensitive liquid biopsy of circulating extracellular vesicles using ExoScreen.	Yoshioka, Y., Kosaka, N., Konishi, Y., Ohta, H., Okamoto, H., Sonoda, H., Nonaka, R., Yamamoto, H., Ishii, H., Mori, M., Furuta, K., Nakajima, T., Hayashi, H., Sugisaki, H., Higashimoto, H., Kato, T., Takeshita, F., Ochiya, T.	Nat. Commun.	2014年	国外
CD10 as a novel marker of therapeutic resistance and cancer stem cells in head and neck squamous cell carcinoma.	Fukusumi, T., Ishii, H., Konno, M., Yasui, T., Nakahara, S., Takenaka, Y., Yamamoto, Y., Nishikawa, S., Kano, Y., Ogawa, H., Hasegawa, S., Hamabe, A., Haraguchi, N., Doki, Y., Mori, M., Inohara, H.	Br. J. Cancer	2014年	国外
MicroRNA-1246 expression associated with CCNG2-mediated chemoresistance and stemness in pancreatic cancer.	Hasegawa, S., Eguchi, H., Nagano, H., Konno, M., Tomimaru, Y., Wada, H., Hama, N., Kawamoto, K., Kobayashi, S., Nishida, N., Koseki, J., Nishimura, T., Gotoh, N., Ohno, S., Yabuta, N., Nojima, H., Mori, M., Doki, Y., Ishii, H.	B.r J. Cancer	2014年	国外
Combined evaluation of hexokinase 2 and phosphorylated pyruvate dehydrogenase-E1α in invasive front lesions of colorectal tumors predicts cancer metabolism and patient prognosis.	Hamabe, A., Hirofumi, Y., Konno, M., Uemura, M., Nishimura, J., Hata, T., Takemasa, I., Mizushima, T., Nishida, N., Kawamoto, K., Koseki, J., Doki, Y., Mori, M., Ishii, H.	Cancer Sci.	2014年	国外
Role of pyruvate kinase M2 in transcriptional regulation leading to epithelial-mesenchymal transition.	Hamabe, A., Konno, M.,Tanuma, N., Shima, H., Tsunekuni, K., Kawamoto, K., Nishida, N., Koseki, J.,Mimori, K., Gotho, N., Yamamoto, H., Doki, Y., Mori, M., Ishii, H.	Proc. Natl. Acad. Sci. U S A.	2014年	国外
Antibody fragment-conjugated polymeric micelles incorporating platinum drugs for targeted therapy of pancreatic cancer.	Ahn, J., Miura, Y., Yamada, N., Chida, T., Liu, X., Kim, A., Sato, R., Tsumura, R., Koga, Y., Yasunaga, M., Nishiyama, N., Matsumura, Y., Cabral, H., Kataoka, K.	Biomaterials.	2015年	国外
Precise engineering of siRNA delivery vehicles to tumors using polyion complexes and gold nanoparticles.	Kim, HJ., Takemoto, H., Yi, Y., Zheng, M., Maeda, Y., Chaya, H., Hayashi, K., Mi, P., Pittella, F., Christie, RJ., Toh, K., Matsumoto, Y., Nishiyama, N., Miyata, K., Kataoka, K.	ACS Nano.	2014年	国外
Fine-tuning of charge-conversion polymer structure for efficient endosomal escape of siRNA-loaded calcium phosphate hybrid micelles.	Maeda, Y., Pittella, F., Nomoto, T., Takemoto, H., Nishiyama, N., Miyata, K., Kataoka, K.	Macromol Rapid Commun.	2014年	国外
Actively-targeted polyion complex micelles stabilized by cholesterol and disulfide cross-linking for systemic delivery of siRNA to solid tumors.	Oe, Y., Christie, RJ., Naito, M., Low, SA., Fukushima, S., Toh, K., Miura, Y., Matsumoto, Y., Nishiyama, N., Miyata, K., Kataoka, K.	Biomaterials.	2014年	国外
Systemic siRNA delivery to a spontaneous pancreatic tumor model in transgenic mice by PEGylated calcium phosphate hybrid micelles.	Pittella, F., Cabral, H., Maeda, Y., Mi, P., Watanabe, S., Takemoto, H., Kim, HJ., Nishiyama, N., Miyata, K., Kataoka, K.	J Control Release.	2014年	国外
Macrophage-derived reactive oxygen species suppress miR-328 targeting CD44 in cancer cells and promote redox adaptation.	Ishimoto, T., Sugihara, H., Watanabe, M., Sawayama, H., Iwatsuki, M., Baba, Y., Okabe, H., Hidaka, K., Yokoyama, N., Miyake, K., Yoshikawa, M., Nagano, O., Komohara, Y., Takeya, M., Saya, H., Baba, H.	Carcinogenesis.	2014年	国外
Expression of TNF-α and CD44 is implicated in poor prognosis, cancer cell invasion, metastasis and resistance to the sunitinib treatment in clear cell renal cell carcinomas.	Mikami, S., Mizuno, R., Kosaka, T., Saya, H., Oya, M., Okada, Y.	Int J Cancer	2015年	国外
Impacts of CD44 knockdown in cancer cells on tumor and host metabolic systems revealed by quantitative imaging mass spectrometry.	Ohmura, M., Hishiki, T., Yamamoto, T., Nakanishi, T., Kubo, A., Tsuchihashi, K., Tamada, M., Toue, S., Kabe, Y., Saya, H., Suematsu, M.	Nitric Oxide.	2014年	国外
Challenges and strategies for pulmonary delivery of microRNA-based therapeutics.	Fujita,Yu., Kuwano, K., Ochiya, T.	MicroRNAs: Key Regulators of Oncogenesis	2014年	

MicroRNA binding to the HIV-1 Gag protein inhibits Gag assembly and virus production.	Chen, AK., Sengupta, P., Waki, K., Van, Engelenburg, SB., Ochiya, T., Ablan, SD., Freed, EO., Lippincott-Schwartz, J.	Proc Natl Acad Sci U S A.	2014年	国外
Clinical relevance and therapeutic significance of microRNA-133a expression profiles and functions in malignant osteosarcoma-initiating cells.	Fujiwara, T., Katsuda, T., Hagiwara, K., Kosaka, N., Yoshioka, Y., Takahashi, RU., Takeshita, F., Kubota, D., Kondo, T., Ichikawa, H., Yoshida, A., Kobayashi, E., Kawai, A., Ozaki, T., Ochiya, T.	Stem Cells.	2014年	国外
Circulating microRNAs in sarcoma: potential biomarkers for diagnosis and targets for therapy	Fujiwara, T., Kawai, A., Nezu, Y., Fujita, Y., Kosaka, N., Ozaki, T., Ochiya, T.	Chemotherapy	2014年	国外
RPN2 gene confers osteosarcoma cell malignant phenotypes and determines clinical prognosis	Fujiwara, T., Takahashi, RU., Kosaka, N., Nezu, Y., Kawai, A., Ozaki, T., Ochiya, T.	Mol Ther Nucleic Acids.	2014年	国外
Physiological and pathological relevance of secretory microRNAs and a perspective on their clinical application.	Katsuda, T., Ikeda, S., Yoshioka, Y., Kosaka, N., Kawamata, M., Ochiya, T.	Biol Chem.	2014年	国外
Exosomes from bone marrow mesenchymal stem cells contain a microRNA that promotes dormancy in metastatic breast cancer cells.	Ono, M., Kosaka, N., Tominaga, N., Yoshioka, Y., Takeshita, F., Takahashi, RU., Yoshida, M., Tsuda, H., Tamura, K., Ochiya, T.	Sci Signal.	2014年	国外
Circulating microRNAs in drug safety assessment for hepatic and cardiovascular toxicity: the latest biomarker frontier?	Osaki, M., Kosaka, N., Okada, F., Ochiya, T.	Mol Diagn Ther.	2014年	国外
The role of microRNAs in the regulation of cancer stem cells.	Takahashi, RU., Miyazaki, H., Ochiya, T.	Front Genet.	2014年	国外
Premature termination of reprogramming in vivo leads to cancer development through altered epigenetic regulation.	Ohnishi K, Semi K, Yamamoto T, Shimizu M, Tanaka A, Mitsunaga K, Okita K, Osafune K4, Arioka Y, Maeda T, Soejima H, Moriwaki H, Yamanaka S, Woltjen K, Yamada Y.	Cell.	2014年	国外
Concise review: dedifferentiation meets cancer development: proof of concept for epigenetic cancer.	Yamada Y, Haga H, Yamada Y.	Stem Cells Transl Med.	2014年	国外
Application of iPS cell technology to cancer epigenome study: uncovering the mechanism of cell status conversion for drug resistance in tumor.	Matsuda Y, Semi K, Yamada Y.	Pathol Int.	2014年	国外
Epigenetic regulation leading to induced pluripotency drives cancer development in vivo.	Ohnishi K, Semi K, Yamada Y.	Biochem Biophys Res Commun.	2014年	国外
不完全な初期化によるエピゲノム発がん	大西 紘太郎、蝉 克憲、山田 泰広	実験医学	2014年	国内
リプログラミング技術を用いたがんエピゲノム研究	蝉 克憲、山田 泰広	実験医学	2014年	国内
がん幹細胞	河村真吾、山田泰広	実験医学	2015年	国内

ARTICLE

Ultra-sensitive liquid biopsy of circulating extracellular vesicles using ExoScreen

Yusuke Yoshioka[1,2,3], Nobuyoshi Kosaka[1], Yuki Konishi[1,4], Hideki Ohta[5], Hiroyuki Okamoto[5], Hikaru Sonoda[5], Ryoji Nonaka[6], Hirofumi Yamamoto[6], Hideshi Ishii[7], Masaki Mori[6], Koh Furuta[8], Takeshi Nakajima[9], Hiroshi Hayashi[4], Hajime Sugisaki[4], Hiroko Higashimoto[4], Takashi Kato[2], Fumitaka Takeshita[1] & Takahiro Ochiya[1]

Cancer cells secrete small membranous extracellular vesicles (EVs) into their micro-environment and circulation. Although their potential as cancer biomarkers has been promising, the identification and quantification of EVs in clinical samples remains challenging. Here we describe a sensitive and rapid analytical technique for profiling circulating EVs directly from blood samples of patients with colorectal cancer. EVs are captured by two types of antibodies and are detected by photosensitizer-beads, which enables us to detect cancer-derived EVs without a purification step. We also show that circulating EVs can be used for detection of colorectal cancer using the antigen CD147, which is embedded in cancer-linked EVs. This work describes a new liquid biopsy technique to sensitively detect disease-specific circulating EVs and provides perspectives in translational medicine from the stand-point of diagnosis and therapy.

[1] Division of Molecular and Cellular Medicine, National Cancer Center Research Institute, Chuo-ku, Tokyo 104-0045, Japan. [2] Integrative Bioscience and Biomedical Engineering, Graduate School of Advanced Science and Engineering, Waseda University, Shinjuku, Tokyo 162-8480, Japan. [3] Research Fellow of the Japan Society for the Promotion of Science (JSPS), Chiyoda-Ku, Tokyo 102-0083, Japan. [4] R&D Department, SRL Inc., Hino-shi, Tokyo 191-0002, Japan. [5] Diagnostics Division, Shionogi & Co., LTD., Settsu-shi, Osaka 566-0022, Japan. [6] Department of Gastroenterological Surgery, Graduated School of Medicine, Osaka University, Suita, Osaka 565-0871, Japan. [7] Department of Frontier Science for Cancer and Chemotherapy, Osaka University, Graduate School of Medicine, Suita, Osaka 565-0871, Japan. [8] Division of Clinical Laboratories, National Cancer Center Hospital, Chuo-ku Tokyo, 104-0045, Japan. [9] Endoscopy Division, National Cancer Center Hospital, Chuo-ku, Tokyo 104-0045, Japan. Correspondence and requests for materials should be addressed to T.O. (email: tochiya@ncc.go.jp).

ancer cells secrete various types of humoral factors into their microenvironment that are biomarkers for disease diagnosis and prognosis, including cytokines, chemokines and nucleic acids. Extracellular vesicles (EVs), including exosome and microvesicles from cancer cells, have also been found in the blood of cancer patients[1-7] and therefore provide a novel type of biomarker for various patient scenarios.

EVs are small membranous vesicles that differ in their cellular origin, abundance and biogenesis[8], and are naturally secreted by almost all cell types to transport bioactive molecules intercellularly. EVs are positive for tetraspanin family proteins, such as CD63, CD81 and CD9 (refs 9–11), and contain cell surface proteins as well as both mRNA and microRNA[12]. Conventional methods of analyzing EVs generally require large quantities of EVs to be concentrated and processed via time-consuming immunoblotting or enzyme-linked immunosorbent assay (ELISA) assays; these methods are impractical in most clinical settings. In this study, we establish a highly sensitive and rapid analytical technique for profiling surface proteins in EVs

from patient blood that can be used to identify biomarkers of colorectal cancer, named ExoScreen. ExoScreen could monitor circulating EVs in serum without the need for purification step. In addition, we show that ExoScreen is superior for the detection of EVs to conventional methods, immunoblotting and ELISA. Furthermore, we find that ExoScreen enables to detect CD147 and CD9 double-positive EVs, which is abundantly secreted from colorectal cancer cells, in serum from colorectal cancer patients. Our results demonstrate that ExoScreen can be a tool for detection of EVs from as little as 5 µl of cancer patients' serum to detect circulating cancer-derived EVs.

Results

Establishment of ExoScreen to detect EVs in serum. To realize the usage of EVs in clinical situation, we develop methods that specifically detect circulating EVs in the serum based on an amplified luminescent proximity homogeneous assay using photosensitizer-beads[13] without a purification step of EVs
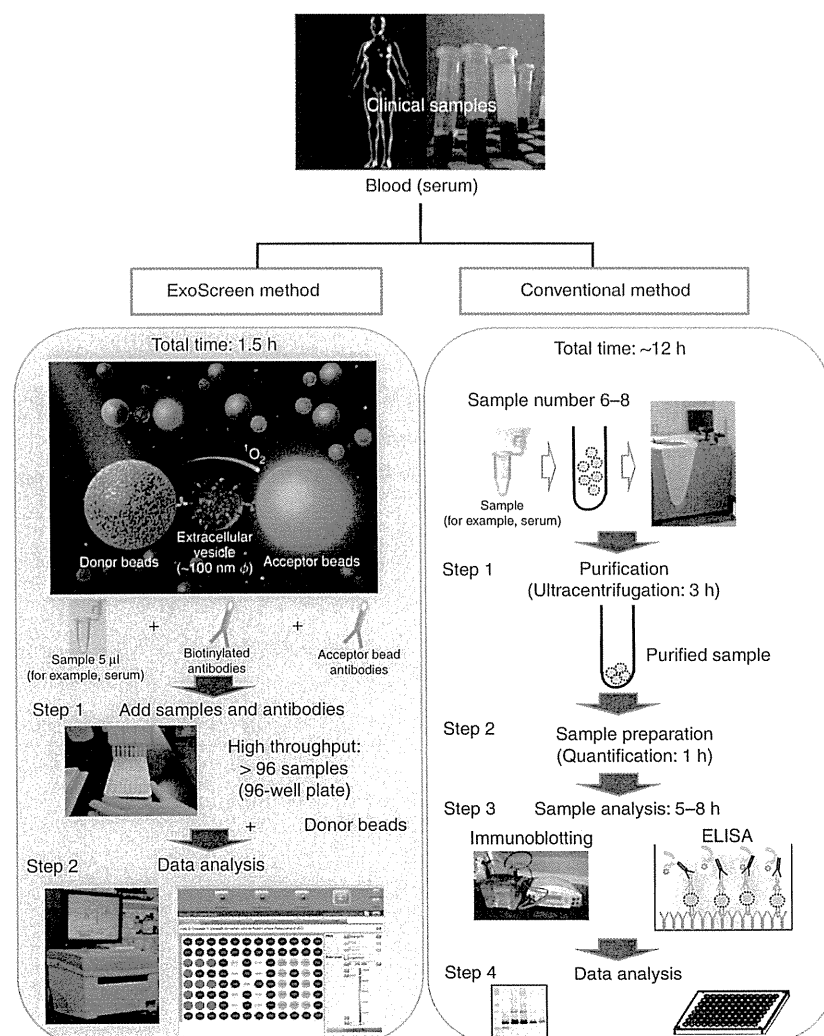
Figure 1 | Schematic overview depicting the method for detecting circulating EVs via conventional methods and ExoScreen. In the case of conventional methods, nearly 12 h are needed to detect the expression of certain protein in circulating EVs. In addition, excessive volumes of serum are required. Conversely, ExoScreen is completed within 2 h and requires only 5 µl of serum. In this system, streptavidin-coated donor beads capture an analyte-specific biotinylated antibody and are used in conjunction with acceptor beads conjugated to a second antibody. The streptavidin-coated donor beads are excited with a laser at 680 nm, resulting in the release of singlet oxygen, which excites an amplified fluorescent signal in the acceptor bead that emits at 615 nm when the beads are within 200 nm of the captured analyte.

—46—
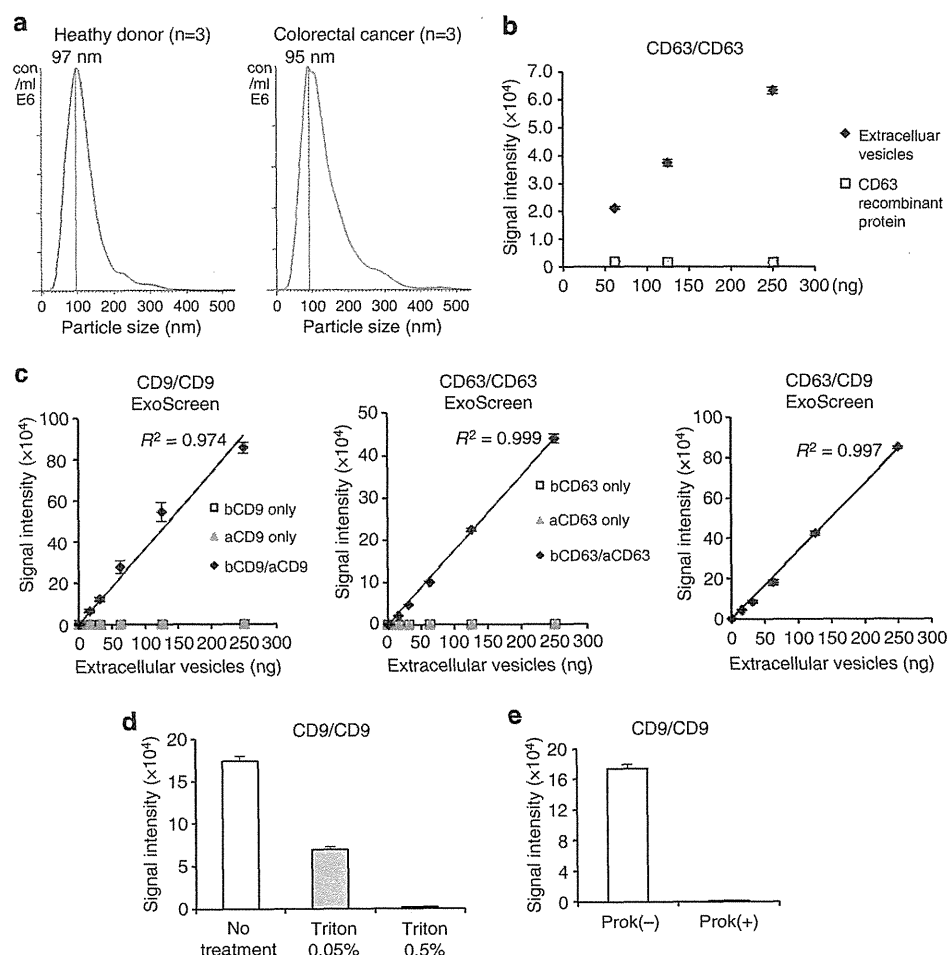
Figure 2 | Establishment of ExoScreen to detect the EVs. (a) Analysis of the size distribution in the serum of healthy donors ($n = 3$) and colorectal cancer patients ($n = 3$) by the NanoSight nanoparticle tracking system. (b) Detection of EVs or monomeric recombinant CD63 protein by ExoScreen using a CD63 antibody. EV protein concentration was measured via the Qubit system. The concentration of recombinant CD63 was adjusted with that of protein in EVs purified from HCT116 CM. Error bars are s.e.m. ($n = 3$ for each condition). (c) Correlation between ExoScreen measurements for CD9 positive EVs, CD63 positive EVs or CD63/CD9 double-positive EVs and EV protein concentration in a dilution series. EV protein concentration was measured via the Qubit system. EVs were purified from HCT116 cell CM. The addition of biotinylated CD9 or CD63 antibodies without acceptor beads conjugated to antibodies is denoted 'bCD9 only' or 'bCD63 only', while 'aCD9 only' or 'aCD63 only' means addition of only acceptor beads conjugated to CD9 or CD63 antibodies without biotinylated antibodies. The addition of biotinylated antibodies and acceptor beads conjugated antibodies is denoted 'bCD9/aCD9' or 'bCD63/aCD63'. Right panel shows the addition of biotinylated CD63 antibodies and acceptor beads conjugated CD9 antibodies. Error bars are s.e.m. ($n = 3$ for each condition). (d) Evaluation of ExoScreen specificity against purified EVs from HCT116 cell treated with or without 0.05% and 0.5% Triton X-100. Two hundred fifty ng of EVs were detected by ExoScreen using CD9 antibodies. Error bars are s.e.m. ($n = 3$ for each condition). (e) Evaluation of ExoScreen specificity against EVs from HCT116 cells treated with (Prok(+)) or without (Prok(−)) Proteinase K. Two hundred fifty ng of EVs were detected by ExoScreen using CD9 antibodies. Error bars are s.e.m. ($n = 3$ for each condition). Data are representative of at least three independent experiments each.

(Fig. 1). This system utilizes streptavidin-coated donor beads to capture an analyte-specific biotinylated antibody, and acceptor beads conjugated to a second antibody that recognizes an epitope of the analyte. The donor beads are excited with a laser at 680 nm, resulting in the release of singlet oxygen, which excites an amplified fluorescent signal in the acceptor beads. As a result, the acceptor beads emit light at 615 nm, but only if they are within 200 nm of the analyte captured by both antibodies. As shown in Fig. 2a, the size of EVs measured by the Nanosight particle tracking system was approximately 100 nm, which prevented the detection of larger vesicles, such as apoptotic bodies, shedding vesicles or protein complexes. In addition, we could not obtain signals from CD63 recombinant protein by ExoScreen, indicating that this assay does not detect antigen monomers (Fig. 2b). We call this assay 'ExoScreen' because the target of the assay is EVs

and because it has a possibility to screen for biomarker of various diseases.

To confirm the reliability for detecting EVs by ExoScreen, we selected CD9 and CD63, which are abundant on the surface of EVs and are expressed in numerous cells, to detect EVs. Conditioned medium (CM) of prostate cancer, prostate epithelial, breast cancer and colorectal cancer cell lines were processed to obtain purified EVs. ExoScreen was able to quantify the amount of EVs present in cell culture supernatants with CD9 and CD63 positive EVs detectable in a dose-dependent manner (Fig. 2c and Supplementary Fig. 1). The negative controls, represented by only the biotinylated antibody or acceptor bead-conjugated antibody, resulted in a minimal fluorescent signal (Fig. 2c). In addition, the signal was decreased after detergent treatment (Fig. 2d and Supplementary Fig. 2) or Proteinase K treatment (Fig. 2e and

−47−
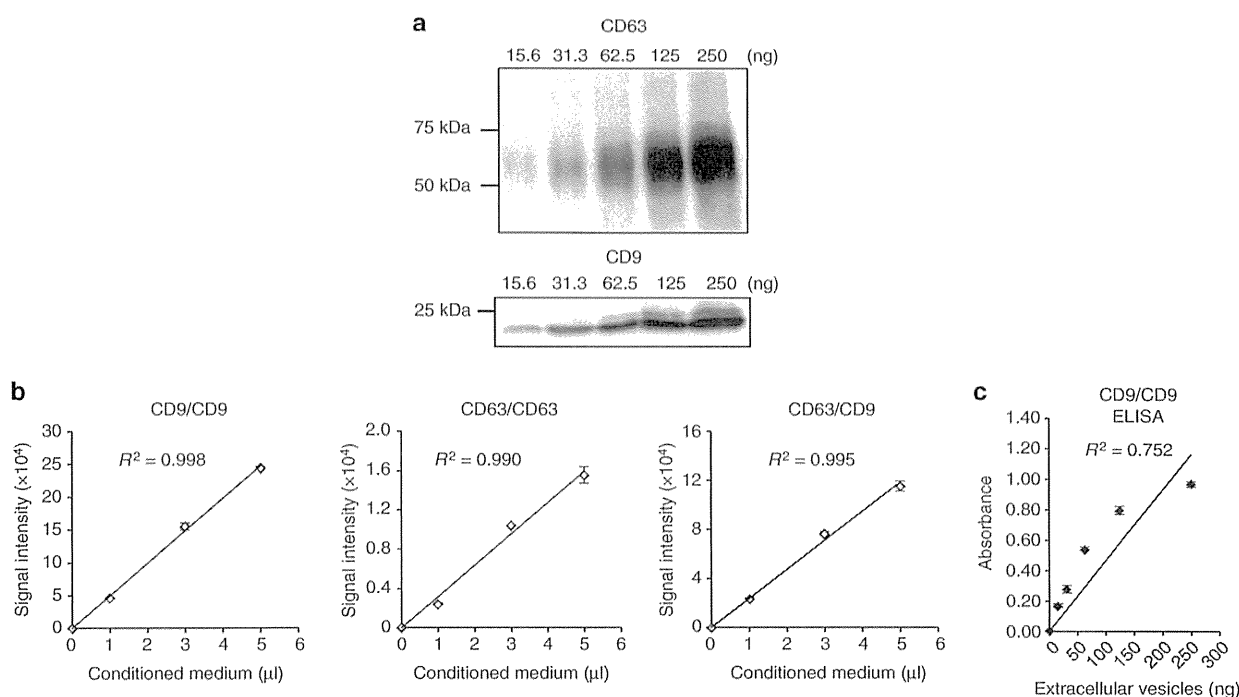
Figure 3 | Comparison of ExoScreen and conventional methods. (**a**) Immunoblotting analysis of CD63 (upper panels) or CD9 (lower panels) against the EVs isolated from HCT116 cells. EV protein concentration were measured via the Qubit system. EVs were purified from HCT116 cell CM. (**b**) Correlation between ExoScreen measurements for CD9 positive, CD63 positive or CD63/CD9 double-positive EVs and HCT116 cell CM in a dilution series. CM was prepared for 5 μl and diluted as indicated. Error bars are s.e.m. ($n = 3$ for each condition). (**c**) Correlation between ELISA measurements for CD9 positive EVs and EV protein concentration in a dilution series. EV protein concentration were measured via the Qubit system. EVs were purified from HCT116 cell CM. Error bars are s.e.m. ($n = 3$ for each condition). Data are representative of at least three independent experiments each.

Table 1 | Comparison of ExoScreen and ELISA.

	ExoScreen	**ELISA**
Incubation time	1.5–3 h	3–6 h + coating time
Steps	2	More than 5
Washes	No	Yes
Throughput	High	Low
Sample volume	Less than 5 μl*	50–200 μl[†]
The volume of antibodies	Low	High
Dynamic range	3–4 logs	2 logs
Analytic range[‡]	3 orders of magnitude	2 orders of magnitude
Sensitivity	High	High
Plate format	96-well or 384-well	96-well

ELISA, enzyme-linked immunosorbent assay.
*Total assay volume 50 μl.
†Total assay volume 200 μl.
‡Calculated by CD9/CD9 analysis of EVs derived from HCT116 cells

Supplementary Fig. 3), indicating that ExoScreen detected complexes of membranous vesicle and transmembrane proteins. Immunoblotting of the same purified EVs preparations confirmed the data obtained by ExoScreen. In fact, CD9 and CD63 proteins were detectable via immunoblotting (Fig. 3a and Supplementary Fig. 4). As shown in Fig. 3a, approximately 32 ng of EV proteins were needed to properly detect CD63 by immunoblotting, while ExoScreen could detect 15.6 ng of purified EVs (Fig. 2c). Furthermore, EVs from only 1 μl of culture medium are enough to detect by ExoScreen (Fig. 3b and Supplementary Fig. 5). In addition, ExoScreen has a wide working range compared with ELISA (Figs 2c and 3c). Moreover, because ExoScreen is a mix-and-read assay, these conventional methods require many steps and substantial time compared with

ExoScreen (Fig. 1). Thus, the ExoScreen assay increases throughput while substantially decreasing hands-on. Taken together, these results indicate that ExoScreen is superior for the detection of EVs to conventional immunoblotting and ELISA (Table 1). The results of EVs detection in culture supernatant without purification (Fig. 3b, Supplementary Figs 5 and 6) prompted us to investigate whether ExoScreen could detect and characterize EVs in human serum. To develop ExoScreen as a diagnostic tool for clinical use, we optimized the method to detect EVs in serum without purification because the protocol exhibited non-linearity of ExoScreen signals against serum samples (Fig. 4a). This non-linearity is most likely a result of the aggregation of condensed proteins in serum. Indeed, we added dextran-500 to suppress serum protein aggregation, and this

−48−
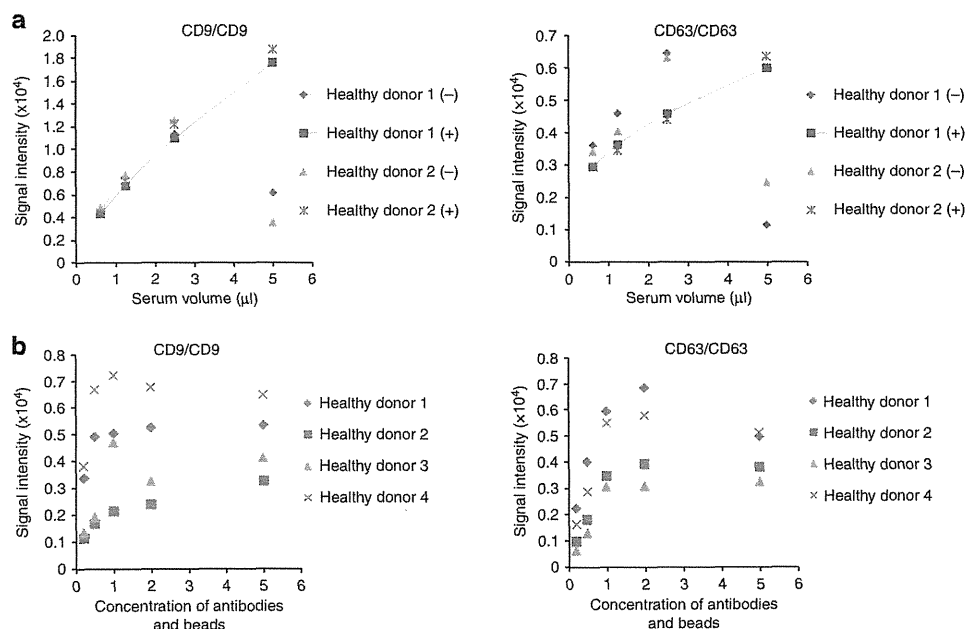
Figure 4 | Detection of circulating EVs in healthy donor sera. (a) Correlation between ExoScreen measurements for CD9 or CD63 and serum volume in a dilution series with (+) or without (−) Dextran-500. The final concentration of Dextran-500 was $1\,mg\,ml^{-1}$. (b) Concentration of '1' means the original concentration of donor and acceptor beads which we used in this study (see Methods section). In addition to original concentration, increased (twofold and fivefold) and decreased (0.5-fold and 0.25-fold) amount of donor and acceptor beads were evaluated by ExoScreen using serum from four healthy donors. Data are representative of at least three independent experiments each.
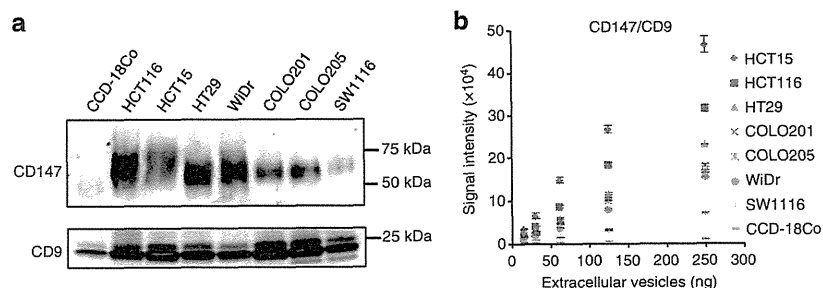
Figure 5 | Analysis of the amount of CD147 in EVs derived from various colon cancer cell lines and a normal colon fibroblast cell line.
(a) Immunoblotting analysis of CD147 or CD9 against purified EVs isolated from CCD-18Co cells, HCT116 cells, HCT15 cells, HT29 cells, WiDr cells, COLO201 cells, COLO205 cells and SW1116 cells. EV proteins (250 ng) was used for the detection of CD147 and CD9. (b) Correlation between ExoScreen detection of CD147/CD9 double-positive EVs and EV protein concentration in a dilution series. EVs protein concentration was measured via the Qubit system. EVs were purified from CCD-18Co, HCT116, HCT15, HT29, WiDr, COLO201, COLO205 or SW1116 CM. Error bars are s.e.m. ($n = 3$ for each condition). Data are representative of at least three independent experiments each.

treatment eliminated the disruption of signals by protein aggregation (Fig. 4a). As shown in Fig. 4a, ExoScreen revealed that serum EVs were captured and expressed both CD9 and CD63 without purification. Further, these signals were detectable in a dose-dependent manner (Fig. 4a). In addition, we assessed whether the concentration of beads, which we employed in this study, was appropriate for the detection of circulating EVs in serum by checking the various concentrations of beads via ExoScreen, and found that the concentration of beads we employed in this study was adequate (Fig. 4b). Taken together, these results indicated that ExoScreen could monitor circulating EVs in serum without the need for a purification process.

Enrichment of CD147 on EVs from colorectal cancer cell lines.
Because EVs are known to represent an important and specific route of intercellular communication[14], we reasoned that tumour-derived EVs may differ from circulating EVs in normal physiological conditions. Previous reports showed that the protein components of EVs from cancer cells were different from normal cells[15,16]. Indeed, it has been recently reported that for patients with stage III melanoma, the amount of specific protein in EVs was significantly increased in individuals who eventually developed metastatic disease, indicating that EVs might have great potential for cancer diagnosis[6]. To identify cancer-derived EVs in cancer patients, EVs derived from the colorectal cancer cell line HCT116 cells and a normal colon fibroblast cell line CCD-18Co cells were subjected to proteomic analysis (Supplementary Table 1). When EVs isolated from CCD-18Co cells were compared with HCT116 cells, the amount of CD147, which is the immunoglobulin superfamily member, was found to be significantly high in the EVs of HCT116 cells, whereas the expression could not be observed in CCD-18Co cells.

−49−
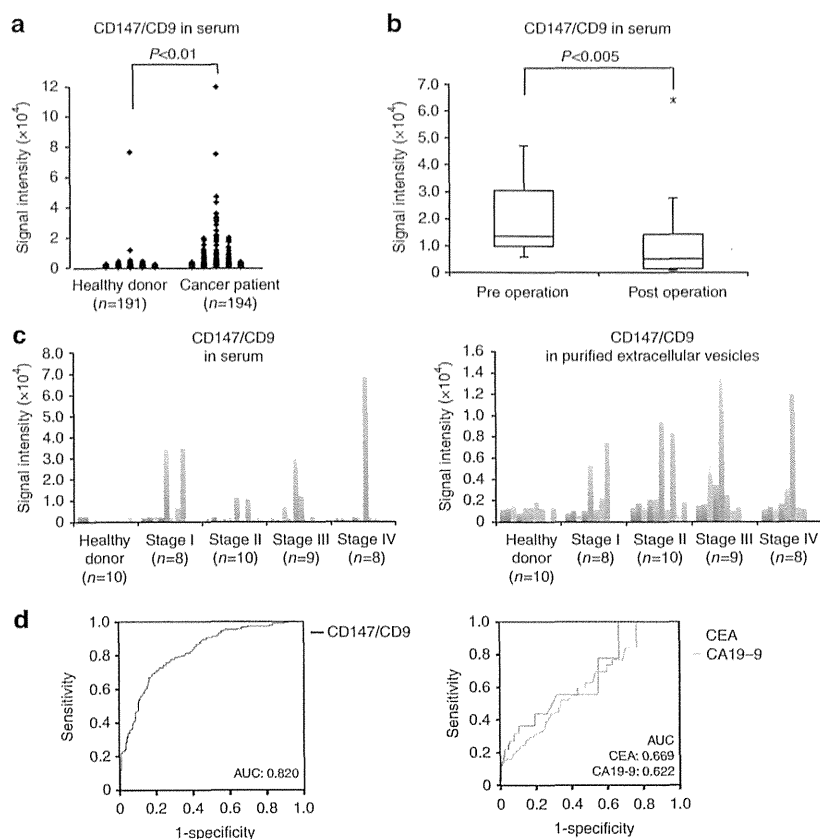
Figure 6 | Analysis of circulating CD147 and CD9 double-positive EVs in healthy donors or colorectal cancer patient sera. (a) Serum levels of CD147/CD9 double-positive EVs in colorectal cancer patients without any purification. The panel shows a scatter plot for healthy donors ($n = 191$) and colorectal cancer patients ($n = 194$). The P-value was calculated by using Wilcoxon rank-sum test. (b) Changes in serum levels of CD147/CD9 double-positive EVs in colorectal cancer patients (stage I or II: $n = 15$) before (preoperation) and after (postoperation after 7–34 days) surgical removal of the tumor. Box lengths represent the interquartile range (first to third quartiles). The line in the center of the boxes represents the median value. Data represented by the asterisks are extreme values (greater than three times the interquartile range over the third quartile). The P-value was calculated by using Wilcoxon signed-rank test. (c) The results of ExoScreen detection of circulating EVs (left panel) and purified circulating EVs (right panel) in sera from healthy donors ($n = 10$) and colorectal cancer patients ($n = 35$) using CD147 and CD9 antibodies. The panels show the signal intensities from each samples measured for CD147/CD9 double-positive EVs using ExoScreen. (d) Receiver operating characteristic curves between healthy donors and colorectal cancer patients assesing by CD147/CD9 double-positive EVs (left panel), CEA and CA19-9 (right panel). left panel, CD147/CD9 double-positive EVs (healthy donors versus colorectal cancer patients; AUC: 0.820); right panel, CEA (AUC: 0.669); CA19-9 (AUC: 0.622) Data are representative of at least three independent experiments each. AUC, area under the curve.

Notably, CD147 is plasma membrane protein and this is suitable for applying to the ExoScreen. We observed that CD147 is expressed on all of the colorectal cancer cell lines, but their expression levels are not uniform (Fig. 5a,b and Supplementary Figs 7 and 8). In addition, CD147 in EVs from CCD-18Co cells was hardly detectable. Several reports have shown that CD147 is expressed in the majority of human tumour types including colorectal cancer[17,18], although CD147 is expressed in a variety of embryonic and adult tissues, such as spermatocytes, neuronal cells, erythrocyte and so on[19]. In addition, CD147 functions in lactate transporter, which is an important feature of cancer cell, because of the excessive anaerobic glycolysis phenomenon in cancer cells referred to as the Warburg effect[20]. Indeed, associations between high expression of CD147 and poor prognosis have previously been shown in colorectal cancer[21], thus representing a potential marker for *ex vivo* analysis of tumour-derived EVs.

CD147 and CD9 double-positive EVs in clinical samples. Next, we used ExoScreen to detect cancer-derived EVs in human clinical samples (Fig. 6a). As shown in Fig. 6a, we found that

CD147 and CD9 double-positive EVs were significantly higher in serum from cancer patients ($n = 194$) than in serum from healthy donors ($n = 191$). Most importantly, most of CD147 in cancer patient sera reduced after surgery (Fig. 6b), suggesting that the reduced signal of CD147 obtained from ExoScreen is originated from cancer-derived EVs, even the variety of cells expressed CD147. To confirm whether by ExoScreen really reflects the protein profile of EVs in circulation, EVs were purified from the sera of tumour patients ($n = 35$) and healthy donors ($n = 10$) and analysed for expression of CD147 via immunoblotting (Supplementary Fig. 9). We also performed ExoScreen against the same serum samples obtained by ultracentrifugation (Fig. 6c, right panel). As depicted in Supplementary Fig. 9, the expression of CD147 in EVs isolated from the sera of cancer patients correlated clearly with the results obtained from the ExoScreen assay (Fig. 6c), indicating that the accuracy of ExoScreen was confirmed and that it can be used to monitor EVs in circulation without any purification. Taken together, these results demonstrate that ExoScreen can be a tool for detection of EVs from as little as 5 μl of cancer patients' serum to detect circulating cancer-derived EVs.

—50—

Discussion

In summary, we propose a rapid, highly sensitive and widely usable detection method based on the amplified luminescent proximity homogeneous assay using photosensitizer-beads for cancer cell-derived EVs. Notably, different antibodies can be conjugated to capture different analytes, such as CD147, thus various types of cancer can be targetd. There are various colorectal cancer screening tests. For example, the fecal occult blood test has been recommended widely as a screening test for colorectal cancer; however, the fecal occult blood displays low sensitivity and specificity for detecting colorectal cancer[22]. Moreover, carcinoembrionic antigen (CEA) and carbohydrate antigen 19-9 (CA19-9) are the most commonly used tumour-associated antigens in the management of patients with colorectal cancer, although those biomarkers are not sensitive enough for early colorectal cancer[23,24]. In fact, the high levels of CD147 detected in patient sera showed the normal value range of CEA and CA19-9 in stage I patients (Supplementary Tables 2 and 3). In addition, the receiver operating characteristic curve indicates a diagnostic advantage of CD147/CD9 double-positive EVs in comparison with CEA and CA19-9 (Fig. 6d). From these aspects and the result shown in Fig. 6b, ExoScreen detecting CD147/CD9 double-positive EVs might be used for monitoring the status of cancer after the surgery and during chemotherapy, resulting in increase in QOL of the patients and providing doctor for the proper assessment of patient status. Further studies are needed to know whether our ExoScreen reduces colorectal cancer mortality as a screening test. It should be noted that CD147/CD9 double-positive EVs were also detected in samples with early stage colorectal cancer that invade into submucosal layer (T1 stage according to UICC classification) (Supplementary Table 2) by the ExoScreen assay. These results also indicate that ExoScreen can be used to detect biomarkers for diseases that are currently difficult to diagnose and monitor not only cancer, but autoimmune disease and degenerative disease of the brain. Thus, our data suggest that ExoScreen, in addition to being a novel liquid biopsy platform for the detection of circulating EVs, may aid variety of disease diagnosis and help to identify companion biomarkers that are important for new drug development.

Methods

Cell cultures. Human colorectal cancer cell lines (HCT116 cells, HCT15 cells, HT29 cells, COLO201 cells, COLO205 cells, WiDr cells and SW1116 cells) and normal colon fibroblast cell line CCD-18Co cells were purchased from American Type Culture Collection. HCT116 and HT29 cells were cultured in McCoy's 5A medium supplemented with 10% heat-inactivated fetal bovine serum (FBS) and an antibiotic–antimycotic solution (Invitrogen) at 37 °C in 5% CO_2. WiDr cells CCD-18Co cells were cultured in minimal essential medium (MEM) containing 2 mM L-gulutamine, an antibiotic–antimycotic solution, nonessential amino acids and 10% FBS at 37 °C in 5% CO_2. HCT15 cells, COLO201 cells and COLO205 cells were cultured in RPMI 1640 medium supplemented with 10% heat-inactivated FBS and an antibiotic–antimycotic solution at 37 °C in 5% CO_2. SW1116 cells were cultured in Leibovitz' L15 medium supplemented with 10% heat-inactivated FBS and an antibiotic–antimycotic solution at 37 °C in without CO_2. The following additional cell lines were used: PNT2 cells, an immortalized normal adult prostatic epithelial cell line (DS Pharma Biomedical Co., Ltd. Osaka, Japan); PC3 cells, a human prostate cancer cell line initiated from a bone metastasis of a grade IV prostatic adenocarcinoma (American Type Culture Collection); MDA-MB-231-luc-D3H2LN cells (MDA-MB-231LN), a highly metastatic human breast cancer cell line (Xenogen); and MCF7 cells, a human breast cancer cell line which expresses oestrogen receptor (American Type Culture Collection). The above cells were cultured in RPMI 1640 medium supplemented with 10% FBS and an antibiotic–antimycotic solution at 37 °C in 5% CO_2.

Patient serum samples. Collection and usage of human serum from corolectal cancer patients ($n = 194$) and healthy donor ($n = 94$) were approved by Osaka university Institutional Review Board (No.11343). Serum was aliquoted and kept at -80 °C until used, and freeze-thawing was avoided as much as possible after that. Some part of the serum samples ($n = 97$) from healthy donor shown in Fig. 6a were purchased from BizCom Japan (Tokyo, Japan). Serum samples containing red

blood cells were excluded from the analysis. Informed consent was obtained from all patients.

Preparation of conditioned media and EVs. The cells were washed with phosphate-buffered saline (PBS), and the culture medium was replaced with advanced Dulbecco's Modified Eagle Medium for HCT116 cells, WiDr cells, SW1116 cells, HT29 cells and CCD-18Co cells, or advanced RPMI medium for the other cell lines, containing an antibiotic–antimycotic and 2 mM L-glutamine (but not containing FBS). After incubation for 48 h, the CM was collected and centrifuged at 2,000 g for 10 min at 4 °C. To thoroughly remove cellular debris, the supernatant was filtered through a 0.22 µm filter (Millipore). The CM was then used for EV isolation. To prepare EVs, CM or the sera from colorectal patients and healthy donors were ultracentrifuged at 110,000 g for 70 min at 4 °C. The pellets were washed with 11 ml of PBS, ultracentrifuged at 110,000 g for 70 min at 4 °C and resuspended in PBS. The putative EVs fraction was measured for its protein content using a Quant-iT Protein Assay with Qubit2.0 Fluorometer (Invitrogen).

Reagents. The following antibodies were used for immunoblotting: mouse monoclonal anti-human CD63 antibody (clone H5C6, dilution 1:200) from BD Biosciences, mouse monoclonal anti-human CD9 antibody (clone ALB 6, dilution 1:200) from SantaCruz Biotechnology, mouse monoclonal anti-human CD147 antibody (clone MEM-M6/1, dilution 1:1,000) from Novus Biologicals and mouse monoclonal anti-Actin (clone C4, dilution 1:1,000) from Millipore. The secondary antibody (horseradish peroxidase-labeled sheep anti-mouse) were purchased from GE HealthCare.

The following antibodies used for ExoScreen and ELISA were developed in Shionogi & Co., LTD.: mouse monoclonal anti-human CD63 antibody (clone 8A12) and mouse monoclonal anti-human CD9 antibody (clone 12A12). Mouse monoclonal anti-human CD147 antibody (clone MEM-M6/1) was purchased from Novus Biologicals. Antibodies were used to modify either acceptor bead or biotin following the manufacturer's protocol.

AlphaLISA reagents (Perkin Elmer, Inc., Waltham, MA 02451, USA) consisted of AlphaScreen Streptavidin-coated donor beads (6760002), AlphaLISA Unconjugated-acceptor beads (6062011) and AlphaLISA Universal buffer (AL001F). AlphaLISA assays were performed in 96-well half-area white plates (6005560) and read in an EnSpire Alpha 2300 Multilabel Plate reader (Perkin Elmer, Inc.).

ExoScreen assay. A 96-well half-area white plate was filled with 5 µl of sample, 5 nM biotinylated antibodies and 50 µg ml^{-1} AlphaLISA acceptor beads conjugated antibodies in the universal buffer. The volume of each reagent was 10 µl. The plate was then incubated for 1–3 h at room temperature. Without a washing step, 25 µl of 80 µg ml^{-1} AlphaScreen streptavidin-coated donor beads were added. The reaction mixture was incubated in the dark for another 30 min at room temperature and the plate was then read on the EnSpire Alpha 2300 Multilabel Plate reader using an excitation wavelength of 680 nm and emission detection set at 615 nm. Background signals obtained from PBS were subtracted from the measured signals.

ELISA. Ninety-six well-plates (Nunc) were coated with 2.5 µg ml^{-1} anti-human CD9 or -CD63 antibodies in a volume of 50 µl per well of carbonate buffer (pH 9.6) and incubated for 4 h at room temperature. After 2 washes with 0.01% Tween-20 in PBS, 100 µl well of Blocking One solution (Nacalai Tesque) was added at room temperature for 1 h. Following 3 washes in PBS, EVs purified from cell culture supernatants were added in a final volume of 50 µl and incubated for 1 h at room temperature. After 3 washes with PBS, 50 µl of biotinylated anti-human CD9 or -CD63 antibodies diluted to 1 µg ml^{-1} were added and incubated for 1 h at room temperature. After 3 washes with PBS, the plate was incubated with 100 µl of HRP-conjugated streptavidin (Cell Signalling Technology) diluted 1:2,000 in Blocking One solution for 1 h at room temperature. After the final 3 washes with PBS, the reaction was developed with Peroxidase (TMB One Component HRP Microwell Substrate, SurModics). The reaction was arrested with 450 nm Stop Reagent for TMB Microwell Substrates (SurModics) and optical densities were recorded at 450 nm.

Immunoblotting. Equal amounts of EVs or whole-cell lysates were loaded onto 4–15% Mini-PROTEAN TGX gels (Bio-Rad, Munich, Germany). Following electrophoresis (100 V, 30 mA), the proteins were transferred to a polyvinylidene difluoride membrane. The membranes were blocked with Blocking One solution and then incubated with primary antibodies. After washing, the membranes were incubated with horseradish peroxidase-conjugated sheep anti-mouse IgG and then subjected to enhanced chemiluminescence using ImmunoStar LD (Wako). CD63, CD9 and CD147 were detected under non-reducing conditions. Original scans of the cropped images in the main figures (Figs 3a and 5a) are presented in Supplementary Fig. 10.

Measurement of size distribution by NTA. Nanoparticle tracking analysis (NTA) was carried out using the Nanosight system (NanoSight) on sera diluted 1000-fold with PBS for analysis. The system focuses a laser beam through a suspension of the particles of interest. These are visualized by light scattering using a conventional optical microscope aligned perpendicularly to the beam axis, which collects light scattered from every particle in the field of view. A 60 s video recorded all events for further analysis by NTA software. The Brownian motion of each particle was tracked between frames to calculate its size using the Stokes–Einstein equation.

References

1. Iero, M. *et al.* Tumour-released exosomes and their implications in cancer immunity. *Cell Death Differ.* **15**, 80–88 (2008).
2. Webber, J., Steadman, R., Mason, M. D., Tabi, Z. & Clayton, A. Cancer exosomes trigger fibroblast to myofibroblast differentiation. *Cancer Res.* **70**, 9621–9630 (2010).
3. Al-Nedawi, K. *et al.* Intercellular transfer of the oncogenic receptor EGFRvIII by microvesicles derived from tumour cells. *Nat. Cell Biol.* **10**, 619–624 (2008).
4. Skog, J. *et al.* Glioblastoma microvesicles transport RNA and proteins that promote tumour growth and provide diagnostic biomarkers. *Nat. Cell Biol.* **10**, 1470–1476 (2008).
5. Taylor, D. D. & Gercel-Taylor, C. MicroRNA signatures of tumor-derived exosomes as diagnostic biomarkers of ovarian cancer. *Gynecol. Oncol.* **110**, 13–21 (2008).
6. Peinado, H. *et al.* Melanoma exosomes educate bone marrow progenitor cells toward a pro-metastatic phenotype through MET. *Nat. Med.* **18**, 883–891 (2012).
7. Kosaka, N., Iguchi, H. & Ochiya, T. Circulating microRNA in body fluid: a new potential biomarker for cancer diagnosis and prognosis. *Cancer. Sci.* **101**, 2087–2092 (2010).
8. Raposo, G. & Stoorvogel, W. Extracellular vesicles: exosomes, microvesicles, and friends. *J. Cell Biol.* **200**, 373–383 (2013).
9. Mathivanan, S. & Simpson, R. J. ExoCarta: a compendium of exosomal proteins and RNA. *Proteomics* **9**, 4997–5000 (2009).
10. Bobrie, A. *et al.* Rab27a supports exosome-dependent and -independent mechanisms that modify the tumor microenvironment and can promote tumor progression. *Cancer Res.* **72**, 4920–4930 (2012).
11. Yoshioka, Y. *et al.* Comparative marker analysis of extracellular vesicles in different human cancer types. *J. Extracell. Vesicles* **2**, doi:10.3402/jev.v2i0.20424 (2013).
12. Valadi, H. *et al.* Exosome-mediated transfer of mRNAs and microRNAs is a novel mechanism of genetic exchange between cells. *Nat. Cell Biol.* **9**, 654–659 (2007).
13. Eglen, R. M. *et al.* The use of AlphaScreen technology in HTS: current status. *Curr. Chem. Genomics* **25**, 2–10 (2008).
14. Kosaka, N. *et al.* Neutral sphingomyelinase 2 (nSMase2)-dependent exosomal transfer of angiogenic microRNAs regulate cancer cell metastasis. *J. Biol. Chem.* **288**, 10849–10859 (2013).
15. Xiao, D. *et al.* Identifying mRNA, microRNA and protein profiles of melanoma exosomes. *PLoS One* **7**, e46874 (2012).
16. Choi, D. S. *et al.* Quantitative proteomics of extracellular vesicles derived from human primary and metastatic colorectal cancer cells. *J. Extracell. Vesicles* **1**, doi:10.3402/jev.v1i0.18704 (2012).
17. Riethdorf, S. *et al.* High incidence of EMMPRIN expression in human tumors. *Int. J. Cancer.* **119**, 1800–1810 (2006).
18. Li, Y. *et al.* HAb18G (CD147), a cancer-associated biomarker and its role in cancer detection. *Histopathology* **54**, 677–687 (2009).
19. Muramatsu, T. & Miyauchi, T. Basigin (CD147): a multifunctional transmembrane protein involved in reproduction, neural function, inflammation and tumor invasion. *Histol. Histopathol.* **18**, 981–987 (2003).
20. Weidle, U. H., Scheuer, W., Eggle, D., Klostermann, S. & Stockinger, H. Cancer-related issues of CD147. *Cancer. Genomics. Proteomics.* **7**, 157–169 (2010).
21. Boye, K. *et al.* EMMPRIN is associated with S100A4 and predicts patient outcome in colorectal cancer. *Br. J. Cancer.* **107**, 667–674 (2012).
22. Ahlquist, D. A. *et al.* Accuracy of fecal occult blood screening for colorectal neoplasia. A prospective study using Hemoccult and HemoQuant tests. *JAMA* **269**, 1262–1267 (1993).
23. Chapman, M. A., Buckley, D., Henson, D. B. & Armitage, N. C. Preoperative carcinoembryonic antigen is related to tumour stage and long-term survival in colorectal cancer. *Br. J. Cancer.* **78**, 1346–1349 (1998).
24. Kuusela, P. *et al.* Comparison of CA 19-9 and carcinoembryonic antigen (CEA) levels in the serum of patients with colorectal diseases. *Br. J. Cancer.* **49**, 135–139 (1984).

Acknowledgements

Author contributions
T.O. originated the concept. Y.Y., N.K. and T.O. carried out the project design. H.Oh., H.Ok. and H.S. developed the antibodies. R.N., H.Y., H.I., M.M., K.F. and T.N provided the serum samples. H.Ha., H.S., H.Hi., F.T. and T.K. assisted with data interpretation. Y.K. and Y.Y. performed the experiments and T.O. supervised the project; Y.Y., N.K. and T.O. contributed to the writing of the manuscript.

Additional information

CD10 as a novel marker of therapeutic resistance and cancer stem cells in head and neck squamous cell carcinoma

T Fukusumi[1,2], H Ishii[2], M Konno[2], T Yasui[1], S Nakahara[1], Y Takenaka[1], Y Yamamoto[1], S Nishikawa[2], Y Kano[2], H Ogawa[3], S Hasegawa[3], A Hamabe[3], N Haraguchi[4], Y Doki[3], M Mori[3] and H Inohara[*,1]

[1]Department of Otorhinolaryngology—Head and Neck Surgery, Osaka University, Graduate School of Medicine, Suita, 2-2 Yamadaoka, Osaka 565-0871, Japan; [2]Department of Frontier Science for Cancer and Chemotherapy, Osaka University, Graduate School of Medicine, Suita, 2-2 Yamadaoka, Osaka 565-0871, Japan; [3]Department of Gastroenterological Surgery, Osaka University, Graduate School of Medicine, Suita, 2-2 Yamadaoka, Osaka 565-0871, Japan and [4]Department of Surgery, Osaka National Hospital, Osaka, Tyuou-ku, 2-1-14 Houenzaka, Osaka 540-0006, Japan

Background: Cancer stem cells (CSCs) are responsible for treatment failure. However, their identification and roles in resistance are not well established in head and neck squamous cell carcinoma (HNSCC).

Methods: Three HNSCC cell lines (FaDu, Detroit562 and BICR6) were treated with cisplatin or radiation. Cell surface antigens were analysed by LyoPlate, a novel cell surface antigen array. The expression levels of antigens highly expressed after treatments were further compared between cisplatin-resistant Detroit562 cells and its parental line. Association of the candidate antigen with CSCs properties, namely sphere formation and *in vivo* tumourigenicity, was also examined.

Results: CD10, CD15s, CD146 and CD282 were upregulated across the treated cell lines, while the increased expression of CD10 was prominent in the cisplatin-resistant cell line. Isolation mediated by FACS revealed that the CD10-positive subpopulation was more refractory to cisplatin, fluorouracil and radiation than the CD10-negative subpopulation. It also showed an increased ability to form spheres *in vitro* and tumours *in vivo*. Moreover, the CD10-positive subpopulation expressed the CSC marker *OCT3/4* at a higher level than that in the CD10-negative subpopulation.

Conclusions: CD10 is associated with therapeutic resistance and CSC-like properties of HNSCC. CD10 may serve as a target molecule in the treatment of refractory HNSCC.

Head and neck squamous cell carcinoma (HNSCC) is the sixth most common malignancy worldwide (Argiris *et al*, 2008). Despite recent advances in its diagnosis and management, long-term survival of patients with HNSCC remains poor (Lo *et al*, 2003). Radiotherapy and chemotherapy initially control tumour growth; however, over time many patients suffer relapse. To improve prognosis, the establishment of a novel marker to predict therapeutic resistance is required. This would also aid the optimisation of HNSCC treatment, and thus benefit patient outcome.

Cancer stem cells (CSCs) are defined as cells that possess the properties of tumour initiation and self-renewal. It is currently understood that CSCs are responsible for treatment failure in a diversity of cancers (Bao *et al*, 2006; Li *et al*, 2008). CD44 (Prince *et al*, 2007) and ALDH1 (Chen *et al*, 2009) have been reported to represent candidate markers of HNSCC CSCs; however, whether they serve as true markers remains controversial (Chen *et al*, 2011; Koukourakis *et al*, 2012). These discrepant reports prompted us to search for a novel marker specific to HNSCC CSCs. Thus, in the present study we aimed to identify a new cell surface antigen that is

---

involved in therapeutic resistance, and to address whether it served as a marker for HNSCC CSCs. Through array analysis and testing of cell viability in the presence of therapeutic agents, we identified CD10 as a potential marker of refractory HNSCC. Moreover, CD10 was found to confer a CSC-like phenotype, and underscored expression of *OCT3/4*. Thus, CD10 could be a specific marker of HNSCC CSCs that contributes to therapeutic resistance.

MATERIALS AND METHODS

Cell culture. FaDu and Detroit562 cell lines were obtained from the ATCC (Manassas, VA, USA), while BICR6 was from ECACC (Proton Down, Salisbury, UK). FaDu and BICR6 were established from a primary hypopharyngeal cancer, while Detroit562 were from a lymph node metastasis of pharyngeal cancer. Cells were cultured in Dulbecco's modified Eagle's medium (DMEM; Sigma Aldrich, St. Louis, MO, USA) supplemented with 10% foetal bovine serum (FBS) and a penicillin (50 U ml^{-1}) and streptomycin (50 μg ml^{-1}) cocktail under an atmosphere of 5% CO_2 at 37 °C. The cisplatin-resistant Detroit562 cell line was established by continuous stepwise exposure to cisplatin starting from a concentration of 1 μM up to 10 μM.

Cell surface antigen arrays. Cells were exposed to 3 μM cisplatin for 7 days. Alternatively, cells were irradiated by a single fraction of 8 Gy and further cultured for 5 days. The expression patterns of cell surface antigens were then compared between the treated and untreated cells using the LyoPlate cell surface antigen array (BD Biosciences, San Jose, CA, USA). The kit consists of three 96-well plates coated with monoclonal antibodies along with AlexaFluor 647 conjugated goat anti-mouse Ig and goat anti-rat Ig secondary antibodies. It allows comprehensive analysis of 242 cell surface antigens by flow cytometry, which was performed using the Cell Analyzer EC800 (Sony, Tokyo, Japan).

Flow cytometry and cell sorting. Flow cytometry and cell sorting were performed using the FACSAria II (BD, Franklin Lakes, NJ, USA). Cells were harvested and single-cell suspensions were prepared with the aid of StemPro Accutase (Life Technologies, Carlsbad, CA, USA). Spheroid cells were separated into single-cell suspensions with the aid of collagenase I (Sigma Aldrich) and adjusted to a concentration of 10^7 cells ml^{-1}. To stain surface antigens, cells were incubated with antibodies against CD10, CD15s, CD44, CD146 and CD282 for 30 min on ice. The fluorophores for each antibody were as follows: CD10—Brilliant Violet (Biolegend, San Diego, CA, USA) and APC (BD Biosciences); CD44—FITC (BD Biosciences); CD146—APC (Biolegend); CD282—PE (BD Biosciences). For CD15s, we combined purified antibody (BD Biosciences) and the secondary antibody—APC/Cy7 (BD Biosciences). The antibodies against CD10, CD15s and the secondary antibody of CD15s were used at a concentration of 50 μl ml^{-1}. The antibodies against CD44, CD146 and CD282 were used at a concentration of 200 μl ml^{-1}. To stain ALDH1, we used the Aldefluor stem cell detection kit (StemCell Technologies, Vancouver, BC, Canada) at a concentration of 50 μl ml^{-1} for 45 min at 37 °C. The fluorophore of Aldefluor was FITC. Doublet cells were eliminated using FSC-A/FSC-H and SSC-A/SSC-H. Dead and damaged cells were eliminated using 7-AAD (BD Biosciences). Briefly, after CD10, CD15s, CD44, CD146, CD282 and ALDH1 staining, 7-AAD was incubated with cells for 10 min at room temperature. Except cell sorting, all FACS analysis was performed three times.

Viability assay. Cells were seeded in 96-well plates at 3 × 10^3 cells per well, cultured overnight and then incubated with 0.1–5 μM cisplatin or 0.5–50 μM fluorouracil for 72 h. Alternatively, cells were irradiated at a single fraction of 8 Gy and then cultured for 72 h.

Cell viability was subsequently measured using the Cell Counting Kit-5 (Dojindo Laboratories, Kamimasiki, Japan). The assay was performed three times.

Sphere formation assay. Cells were seeded in 96-well flat bottom ultra-low attachment culture dishes (Corning, Tewksbury, MA, USA) at 10 cells per well in ReproStem medium (ReproCELL, Yokohama, Japan) containing penicillin (50 U ml^{-1}) and streptomycin (50 μg ml^{-1}) cocktail and basic fibroblast growth factor (5 ng ml^{-1}) without FBS. After 10 days, the size of spheroid colonies was measured under a microscope and the number of colonies with a diameter over 100 μM was counted. The assay was performed three times.

Xenograft assay. The various numbers of cells (1 × 10^2, 1 × 10^3 and 1 × 10^4) were diluted in equal amounts of DMEM and Matrigel (BD Biosciences) to a final volume of 200 μl then injected subcutaneously into NOD/SCID mice (Charles River Laboratories Japan, Yokohama, Japan) using a 22-gauge needle. The mice were maintained under pathogen-free conditions and sacrificed 2 months later or when tumours exceeded 20 mm at the largest diameter. Mice were handled in accordance with the procedures outlined in the Regulations on Animal Experiments at Osaka University. The institutional committee on animal research approved the study.

Quantitative real-time PCR. Quantitative real-time PCR was used to validate siRNA-mediated knockdown of CD10 and to examine mRNA levels of *OCT3/4*. Briefly, total RNA was isolated from cells using TRIzol reagent (Life Technologies) and cDNA was synthesised using the ReverTra Ace qPCR RT Master Mix (Toyobo, Osaka, Japan). Quantitative reverse transcription–PCR (qRT–PCR) was performed using a Light Cycler TaqMan Master (Roche, Basel, Switzerland). The primer sequences were as follows: CD10 5'-GGGGAGGCTTTATGTGGAAG-3' (sense) and 3'-CTC GGATCTGTGCAATCAAA-5' (antisense); and OCT3/4 5'-GAAA CCCACACTGCAGATCA-3' (sense) and 3'-CGGTTACAGAACC ACACTCG-5' (antisense). Gene expression levels were normalised to that of ACTB, 5'-AGAGCTACGAGCTGCCTGAC-3' (sense) and 3'-CGTGGATGCCACAGGACT-5' (antisense).

Transfection. The siRNA duplexes, si-CD10 and si-control, were obtained from Life Technologies. The si-CD10 sequences were as follows: 5'-GGCCCUUUAUGGUACAACCUCAGAA-3' (sense) and 3'-UUCUGAGGUUGUACCAUAAAGGGCC-5' (antisense). An initial dose-response experiment was performed according to the manufacturer's instructions to determine optimal transfection efficiency. Optimal inhibition was observed at a concentration of 10 nM siRNA at 72 h after transfection, thus further qRT–PCR analysis was done under these conditions.

Statistical analysis. The comparison of spheroid colony sizes was made using the Mann–Whitney *U-test*. The analyses of viability curves were made using two-way analysis of variance. Other statistical comparisons were made using the Student's *t*-test. Differences were considered significant when *P* < 0.05. All statistical analyses were performed using JMP Pro 11 (SAS Institute, Cary, NC, USA).

RESULTS

Identification of antigens related to therapeutic resistance. To identify antigens related to therapeutic resistance, surface antigen expression levels in cells from three HNSCC cell lines, Detroit562, FaDu and BICR6 that survived treatment with cisplatin or radiation were compared with those of their untreated counterparts by means of LyoPlate (Supplementary Table 1). From this analysis, four cell surface antigens, CD10, CD15s, CD146 and

CD282, were found to be upregulated in each cell line following either treatment (Table 1).

To further test whether any of these antigens correlated with therapeutic resistance, we established the cisplatin-resistant Detroit562 cell line, which showed excellent viability even in the presence of cisplatin at a concentration as high as 100 μM (Figure 1A). The expression levels of CD10, CD15s, CD146 and CD282 were then compared between the parental and cisplatin-resistant Detroit562. Only CD10 expression levels were found to be significantly upregulated in cisplatin-resistant Detroit562 when compared with those in the parental line. Indeed, the CD10(+) subpopulation accounted for 22.5% compared with 1.4% in cisplatin-resistant Detroit562 and parental cells, respectively (Figure 1B). Of note, interdependence was not detected among the four markers (Figure 1C). These results indicate that CD10 may serve as a cell surface antigen specific to refractory HNSCC cells.

Association of CD10 with chemo and radio resistance. To further address the role of CD10 in resistance, we examined whether the CD10(+) subpopulation was chemo and/or radio resistant. To do this, CD10(+) and CD10(−) subpopulations were isolated by FACS from the FaDu and Detroit562 cell lines, and their viability after cisplatin treatment was compared. As shown in Figure 2A and B, the CD10(+) subpopulation was significantly more refractory to cisplatin than the CD10(−) subpopulation in both FaDu and Detroit562. We also examined whether CD10 affected the sensitivity of cells to fluorouracil, which is used in combination with cisplatin in the treatment of HNSCC (Kish et al, 1982). As shown in Figure 2C and D, the CD10(+) subpopulation was also significantly more refractory to fluorouracil in Detroit562. Next, we investigated the association between CD10 and radiation sensitivity. We found that the CD10(+) subpopulations of both FaDu and Detroit562 were significantly more radio resistant than the respective CD10(−) subpopulations (Figure 2E).

Association between CD10 and the cell cycle. Generally, cisplatin and fluorouracil affect DNA synthesis. Thus, slow-cell cycling or dormant cells (G0/G1 phase) are resistant to these chemotherapeutic agents (Barr et al, 2013). As for radiation, cells are most sensitive to its effects during the G2/M phase and less sensitive in G1/0 and S phases (Sinclair, 1968). We hypothesised that the chemo and radio resistance of the CD10(+) subpopulation was associated with cell cycle phase. Thus, we performed cell cycle analysis using Hoechst33342. As shown Figure 2F-G, the CD10(+) subpopulation had a greater proportion of cells in the G0/G1 phase and less in the G2/M phase than the CD10(-) subpopulation. These data indicated that the CD10(+) subpopulation of HNSCC cells was slow-cell cycling or dormant compared with the CD10(-) subpopulation.

CD10 and sphere formation ability. Given that CSCs are responsible for therapeutic resistance (Bao et al, 2006; Li et al, 2008), and are also in the dormant or slow-growing phase of the cell cycle (Holyoake et al, 1999), we hypothesised that CD10 might be a novel marker for CSCs in HNSCC. One of the most important characteristics of CSCs is self-renewal ability, which is assessed by sphere formation. First, we examined the distribution of CD10 in spheroid cells and control adherent cells using FACS analysis. In FaDu, 10.3% of spheroid cells and 2.1% of adherent cells were CD10(+). Similarly, 10.2% of spheroid cells and 1.7% of adherent cells were CD10(+) in Detroit562 (Figure 3A and B). Next, we compared sphere formation ability between CD10(+) and CD10(-) subpopulations. Although the morphology of spheroid colonies was similar between the two subpopulations (Figure 3C), there was a significant difference in their number. The CD10(+) subpopulation formed more spheroid colonies than the CD10(−) subpopulation in both FaDu and Detroit562 (Figure 3D-E). Moreover, colonies of the CD10(+) subpopulation were larger than those of the CD10(−) subpopulation in FaDu and Detroit562 (Figure 3F-G).

CD10 and tumourigenicity. To further address the association between CD10 and CSC properties, we examined whether CD10 modulates in vivo tumourigenicity. CD10(+) and CD10(−) subpopulations were sorted and individually transplanted into NOD/SCID mice. The result of the limiting dilution transplantation assay of Detroit562 cells is shown in Table 2. Briefly, when 1 000 cells were transplanted, the CD10(+) subpopulation formed tumours in six of six (100%) transplanted mice, while the CD10(-) subpopulation formed tumours in only two of six (33%) mice. Moreover, the CD10(+) subpopulation remained tumourigenic with as few as 100 cells. In contrast, there was no difference in tumourigenicity between the CD10(+) and CD10(−) subpopulations of FaDu (Supplementary Table 2), although the size of tumours formed by inoculation of 1000 cells was notably larger in the CD10(+) subpopulation than in the CD10(−) subpopulation (Supplementary Figure 1). To confirm that the histology of tumours was squamous cell carcinoma, we performed H&E staining (Figure 4A). Both FaDu and Detroit562 tumours from CD10(+) and CD10(−) subpopulations presented with squamous cell carcinoma histology and the shapes of these tumour cells were similar to those of parental cell lines.

Interrelations between CD10 and other CSC markers. It has been reported that CD44 (Prince et al, 2007), CD133 (Chiou et al, 2008) and ALDH1 (Chen et al, 2009) are markers of CSCs in HNSCC; thus, we examined the interdependence between CD10 and these markers. Since CD133 is not contained in the cell surface antigen array, we first assessed its expression in treated (cisplatin or radiation) and untreated FaDu cells by flow cytometry as per the conditions used in the array analysis. We found that CD133 expression was barely detectable even after the treatments

Table 1. Differentially expressed cell surface antigens in three HNSCC cell lines, Detroit562, FaDu and BICR6 following treatment with radiation or cisplatin									
	Detroit562			FaDu			BICR6		
Cell surface antigen	Control (%)	RT (%)	CDDP (%)	Control (%)	RT (%)	CDDP (%)	Control (%)	RT (%)	CDDP (%)
CD10	7.5	36.5	31.8	9.5	23.1	24.3	31.2	38.1	57.6
CD15s	40.7	52.6	66.8	25.5	95.6	74.2	58.4	65.5	78.3
CD146	64.5	76.8	89.2	19.6	82.9	37.3	3.7	9.2	15.2
CD282	8.6	26.7	27.6	11.5	98.8	14.3	7.1	25.3	30.3

Abbreviations: CDDP, cisplatin; RT, radiotherapy. Control, no treatment; RT, cells were assayed 5 days after exposure to single fraction 8 Gy irradiation; CDDP, cells were assayed after exposure to 3 μM cisplatin for 7 days. Data represent the percentages of each marker as measured by flow cytometry.
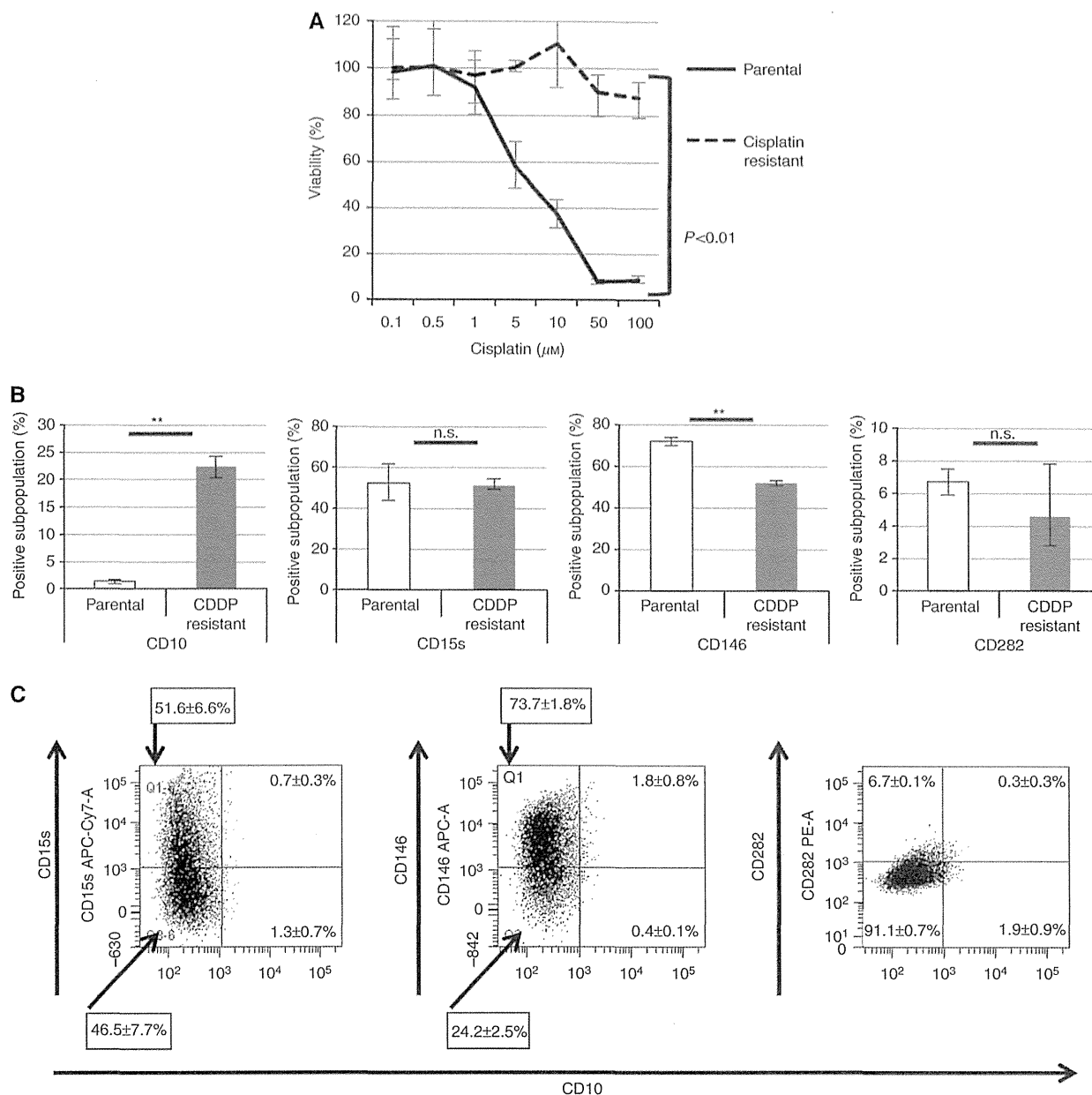
Figure 1. Expressions of candidate antigens in the cisplatin-resistant HNSCC cell line Detroit562. (A) Cisplatin-resistant Detroit562 were generated and validated by testing their viability against that of the parental cell line in response to cisplatin treatment, at the indicated doses. Statistical analysis was performed using two-way analysis of variance. Data represent means ± s.e.m. (B) Expression analyses of CD10, CD15s, CD146 and CD282 by flow cytometry in cisplatin-resistant Detroit562 and the parental cells. The percentages of positive subpopulations are indicated; **$P<0.01$; n.s., not significant. (C) The interdependence of the four markers.

(Supplementary Table 3). Thus a relationship between CD10 and CD133 by means of FACS analysis could not be explored. As for CD44, We found that the majority of FaDu and Detroit562 cells were CD44(+). Although we found that all CD10(+) cells expressed CD44 in both Detroit562 and FaDu cell lines (Supplementary Figure 2A), significant interdependence was not detected. As for ALDH1, we found that CD10(+) cells expressed significantly more ALDH1 than CD10(-) counterparts in both cell lines (Figure 4B and Supplementary Figure 2B). The expression levels of CD10 and ALDH1 were found to be interdependent.

Stem cell-related genes in CD10-positive cells. To shed light on the molecular mechanisms underlying self-renewal ability and tumourigenicity of the CD10(+) subpopulation, we compared the

expression of OCT3/4, a known marker of tissue stem cells (Nichols et al, 1998) and CSCs (Nichols et al, 1998), between CD10(+) and CD10(−) subpopulations. OCT3/4 expression was significantly increased in the CD10(+) subpopulation when compared with that of the CD10(−) subpopulation in both FaDu and Detroit562 (Figure 4C). Of note, knockdown of CD10 by siRNA resulted in decreased expression of OCT3/4 (Figure 4D and Supplementary Figure 3A–B).

DISCUSSION

In the present study, we used the novel cell surface antigens array Lyoplate to identify antigens relevant to cell survival after
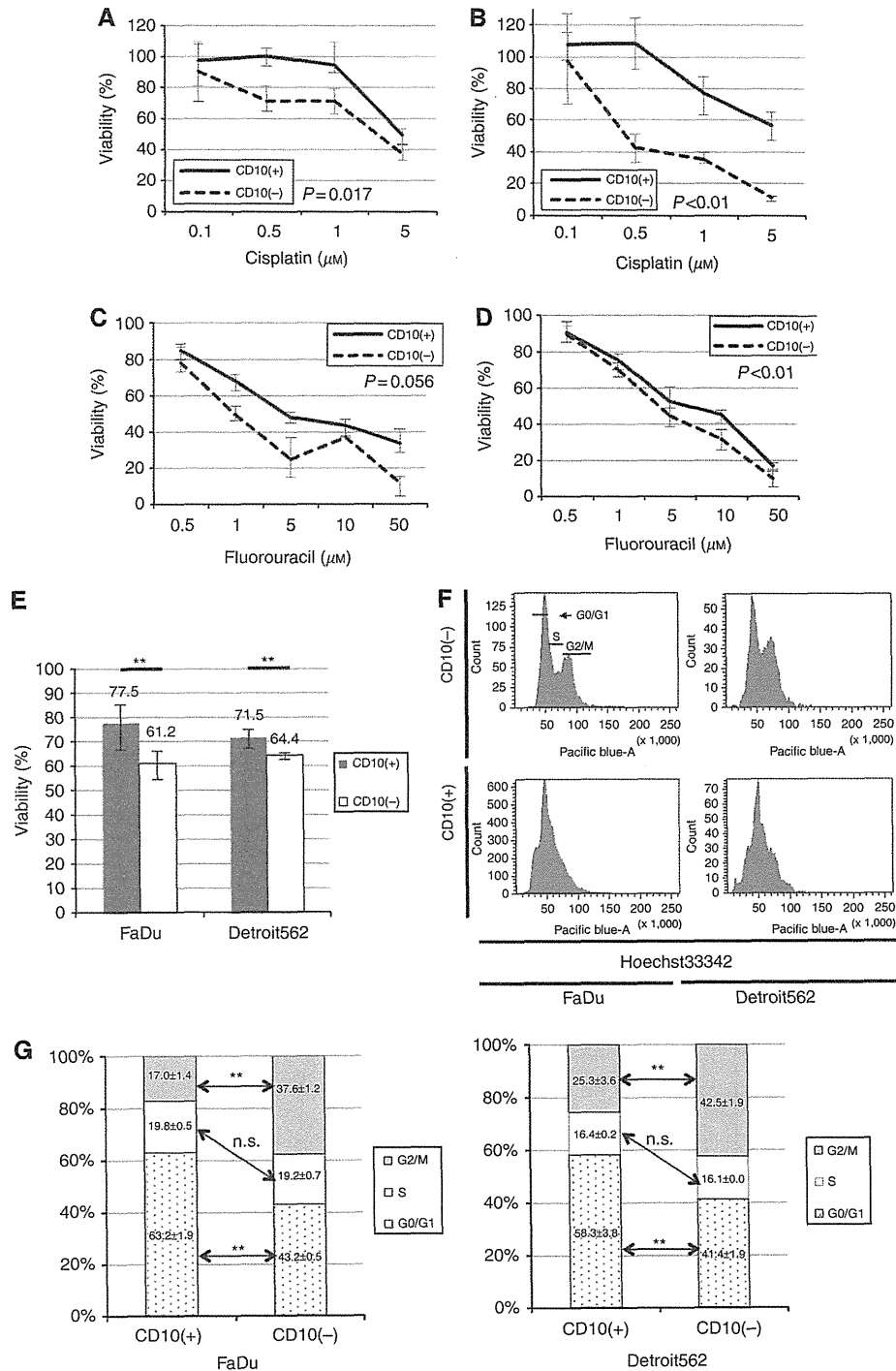
Figure 2. CD10(+)/(−) cell viability in response to treatment with cisplatin, fluorouracil, or radiation and cell cycle analysis. (A–D) CD10(+) and CD10(−) subpopulations were isolated by FACS and cultured with 0.1–5 μM cisplatin or 0.5–50 μM fluorouracil for 72 h. Viability in response to cisplatin in FaDu (A) and Detroit562 (B) or fluorouracil in FaDu (C) and Detroit562 (D) was then measured. Statistical analysis was performed using two-way analysis of variance. (E) Alternatively, cells were exposed to radiation at single fraction 8 Gy. After 72 h, cell viability was measured. Data represent means ± s.e.m.; **$P<0.01$. (F) Cell cycle analysis of CD10-positive and -negative subpopulations was performed after staining with Hoechst33342. (G) The cell cycle phase distribution of CD10 (+)/(−) subpopulations. **$P<0.01$; n.s., not significant.

treatment with cisplatin or radiation. This is the first report that tries to identify an antigen that exhibits both therapeutic resistance and is related to CSCs by means of the cell surface antigens array. We found that CD10, CD15s, CD146 and CD282 were highly expressed in treated cells compared with untreated cells. To validate the result of the cell surface antigens array, we next compared the expression of these antigens between a

cisplatin-resistant cell line and its parental cell line. Of the candidate antigens, only expression of CD10 was upregulated in the cisplatin-resistant cell line as determined by FACS analysis. We propose two reasons for the different antigen expression profiles detected by Lyoplate and FACS analysis. First, different flow cytometers were used for the detection of signals, thus variations in sensitivity may account for the divergent findings.